Microchemical Journal 187 (2023) 108386

Contents lists available at ScienceDirect

Microchemical Journal

journal homepage: www.elsevier.com/locate/microc

Copper ion ratio chemiluminescence probe based on chemiluminescence resonance energy transfer

Xiaomin Liu [a], Jiahui Li [a], Tianquan Wen [c], Zhengpeng Li [d], Xinghua Wang [a], Ming Li [b], Pinyi Ma [a], Daqian Song [a], Qiang Fei [a,*]

[a] College of Chemistry, Jilin Province Research Center for Engineering and Technology of Spectral Analytical Instruments, Jilin University, Qianjin Street 2699, Changchun 130012, China
[b] The National Institute of Metrology, Beijing 100029, China
[c] Pony Testing International Group, Changchun 130103, China
[d] Changchun Gold Research Institute, Changchun 130012, China

ARTICLE INFO

Keywords:
Chemiluminescence resonance energy transfer (CRET)
Ratio detection
CdTe quantum dots (CdTe QDs)
Chemiluminescence (CL)
Cu^{2+}

ABSTRACT

We synthesized the water-soluble CdTe quantum dots (CdTe QDs) with longer emission wavelength, constructed the luminol-CdTe QDs chemiluminescence resonance energy transfer (CRET) system, and realized the high selectivity ratio detection for Cu^{2+}. Herein, based on the Irving-William sequence, it was found that the paramagnetic ion Cu^{2+} generally binds more strongly than the diamagnetic ion Cd^{2+}. When Cu^{2+} is added to the system, Cu^{2+} tends to bind to the sulfhydryl group (S—H) of stabilizer on CdTe QDs, leading to surface defects of CdTe QDs, which quenches the chemiluminescence (CL) signal remarkably. Meanwhile, due to the superior coordination ability of Cu^{2+} and ratio detection, the system has better selectivity and anti-interference performance. The method achieved a highly sensitive, selective, yet reliable measurement of Cu^{2+} in the concentration range of 0.5×10^{-7}-20×10^{-7} M, with a low detection limit of 8.4 nM. Importantly, the sensor has been successfully exploited to detect Cu^{2+} in tap water and lake water.

1. Introduction

Chemiluminescence (CL) is a luminescence phenomenon produced by a chemical reaction, in which various electron excitation intermediates are generated and then return to the ground state emitting light [1,2]. Because CL has many advantages, including the low limit of detection, wide linear range, simple operation, and no interference of background scattered light, it has been applied in many fields, such as clinical diagnosis, biotechnology, heavy metal ion detection, environmental monitoring, food analysis and so on [3,4]. However, single intensity-based CL assays are unstable. Compared with a single signal, ratio detection could remove most of the ambiguity through self-correction [5]. Generally, ratio detection mostly occurs in fluorescence detection, and there are few reports about using CL for ratio detection [6]. Fortunately, chemiluminescence resonance energy transfer (CRET), which is similar to fluorescence resonance Energy transfer (FRET) [7], enables CL to emit at multiple bands, making ratio detection of CL systems possible. Besides, CRET has no external light source, and the non-specific signal triggered by external optical excitation can be minimized compared with FRET [7].

Semiconductor quantum dots (QDs) (e.g. CdTe quantum dots and CdSe quantum dots) due to their excellent photophysical properties, such as broad absorption peaks, large Stokes shifts, narrow and high yield emission bands, and good chemical and optical stability [8], have been used in a variety of detection methods, including atomic fluorescence spectrometry (AFC) [9–11], inductively coupled plasma mass spectrometry (ICP-MC) [9,10], fluorescence (FL) [9,10,12–14] and chemiluminescence (CL) [15,16]. However, the high cost of atomic fluorescence spectrometry (AFC) and inductively coupled plasma mass spectrometry (ICP-MC) hinders their application. Fluorescence (FL) needs an additional light source and background interference is serious, and the single signal chemiluminescence (CL) method also has the disadvantage of signal instability. In this work, we introduce CdTe quantum dots (CdTe QDs) into the CRET system to replace the small molecular fluorophores as the energy acceptor, which greatly improves the efficiency of CRET, and construct a ratio chemiluminescence detection system. The ratio chemiluminescence detection system is not only easy to operate and cheap but also not disturbed by the light source

* Corresponding author.
E-mail address: feiqiang@jlu.edu.cn (Q. Fei).

https://doi.org/10.1016/j.microc.2023.108386
Received 30 September 2022; Received in revised form 12 December 2022; Accepted 2 January 2023
Available online 3 January 2023

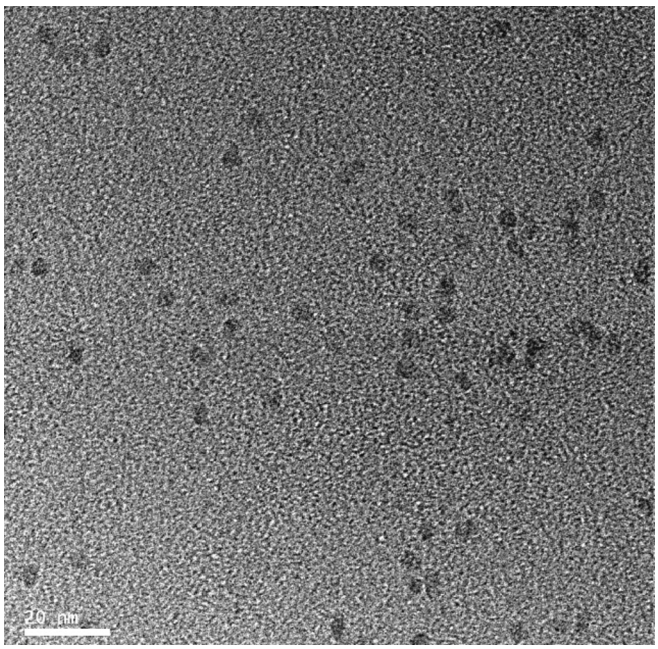

Fig. 1. The TEM image of the synthesized CdTe QDs.

and the ratio signal is more stable.

Copper ions (Cu^{2+}) are essential transition metals for the human body [17] widely distributed in tissues and participate in various biochemical reactions such as catalysis, transport, or biosynthesis [18]. However, high levels of Cu^{2+} may bring a lot of permanent damage to human health, such as liver or kidney damage, Alzheimer's disease, Menkes disease, or Wilson's disease [19]. Inspired by the importance of Cu^{2+} in biological systems, it is necessary to construct a highly sensitive, highly selective, and trace-level detection method of Cu^{2+}.

In this work, the water-soluble CdTe quantum dots (CdTe QDs) with longer emission wavelength (λ_{em} = 733 nm) as CRET receptors have been synthesized and the ratio detection system of Cu^{2+} based on CRET has been constructed. For a long time, the low selectivity of the CL detection method has hindered its application. The ratio detection system of Cu^{2+} we established is based on the Irving-William series [20] and has high selectivity. For the divalent metal ions in the first transition series, the coordination ability of Cu^{2+} is unmatched by other ions, regardless of the properties of ligands and the number of participating ligands [18,21]. At the same time, studies have shown that larger CdTe QDs (4.4 nm) have better selectivity for Cu^{2+} than smaller ones (2.1 nm and 3.3 nm) [22]. Therefore, based on the CRET and the high coordination capacity of Cu^{2+}, the luminol-CdTe QDs system was established to achieve the high selectivity ratio detection of Cu^{2+}, and to some extent overcome the problem of low selectivity of CL.

2. Experimental section

2.1. Chemicals and apparatus

2.1.1. Chemicals and solutions

Luminol was supplied by Sun Chemical Technology Co., ltd. Tellurium (Te) powder (99.999 %) was obtained from Sigma-Aldrich (Shanghai, China). $NaBH_4$ was ordered from Xilong Chemical Co. ltd. *N*-Acetylcysteine (NAC) was obtained from Energy Chemical (Shanghai, China). Horseradish peroxidase (HRP) was purchased from Aladdin

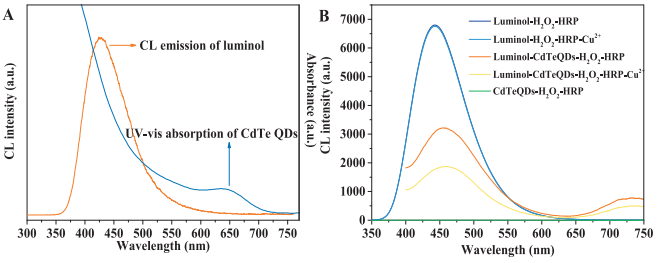

Fig. 3. (A) UV–vis spectrum of CdTe QDs and CL spectrum of luminol. (B) CL spectrum of luminol-H_2O_2-HRP, luminol-H_2O_2-HRP-Cu^{2+}, luminol-CdTe QDs-H_2O_2-HRP, luminol-CdTe QDs-H_2O_2-HRP-Cu^{2+} and CdTe QDs-H_2O_2-HRP (10×10^{-3} mg/mL HRP, 1.6 mM H_2O_2, 0.28 mM luminol, 0.77 μM CdTe QDs and 5×10^{-7} M Cu^{2+}).

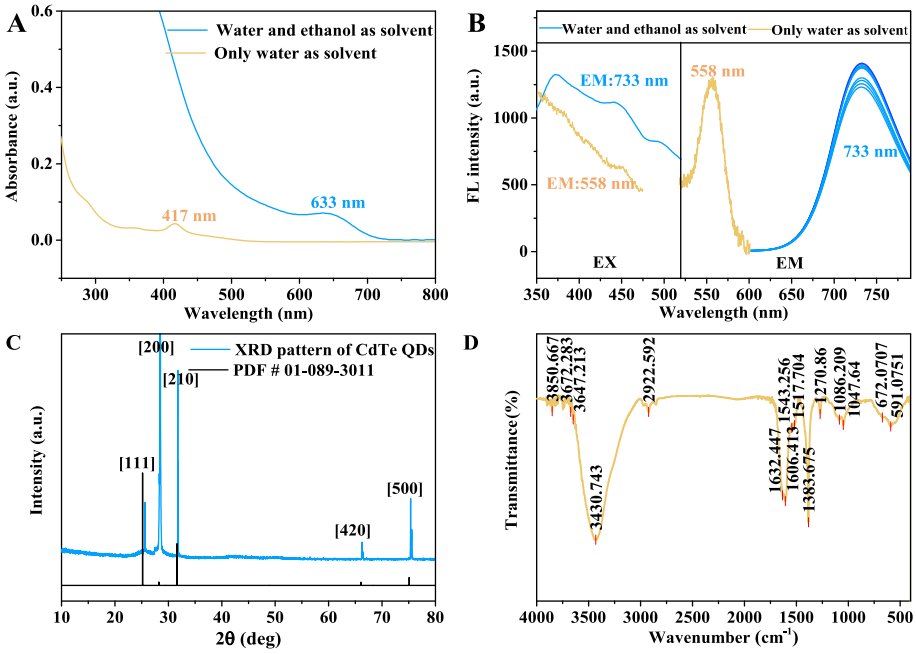

Fig. 2. (A) UV–vis spectra of CdTe QDs prepared with different solvents. (B) FL spectra of CdTe QDs prepared with different solvents. (C) The XRD pattern of the as-synthesized CdTe QDs. (D) The FT-IR spectrum of CdTe QDs.

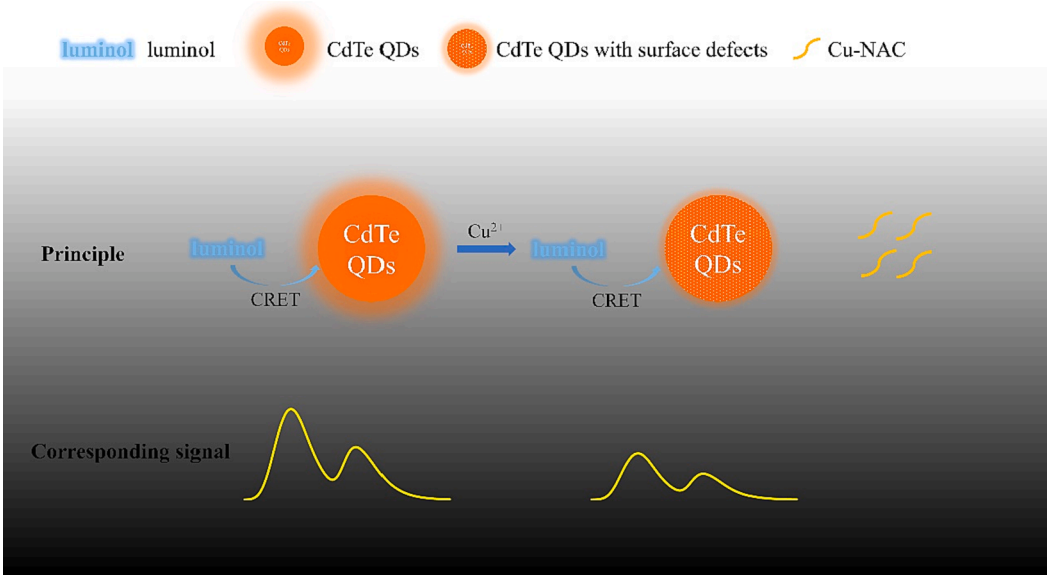

Scheme 1. Illustration of the principle of the ratio detection of Cu^{2+}.

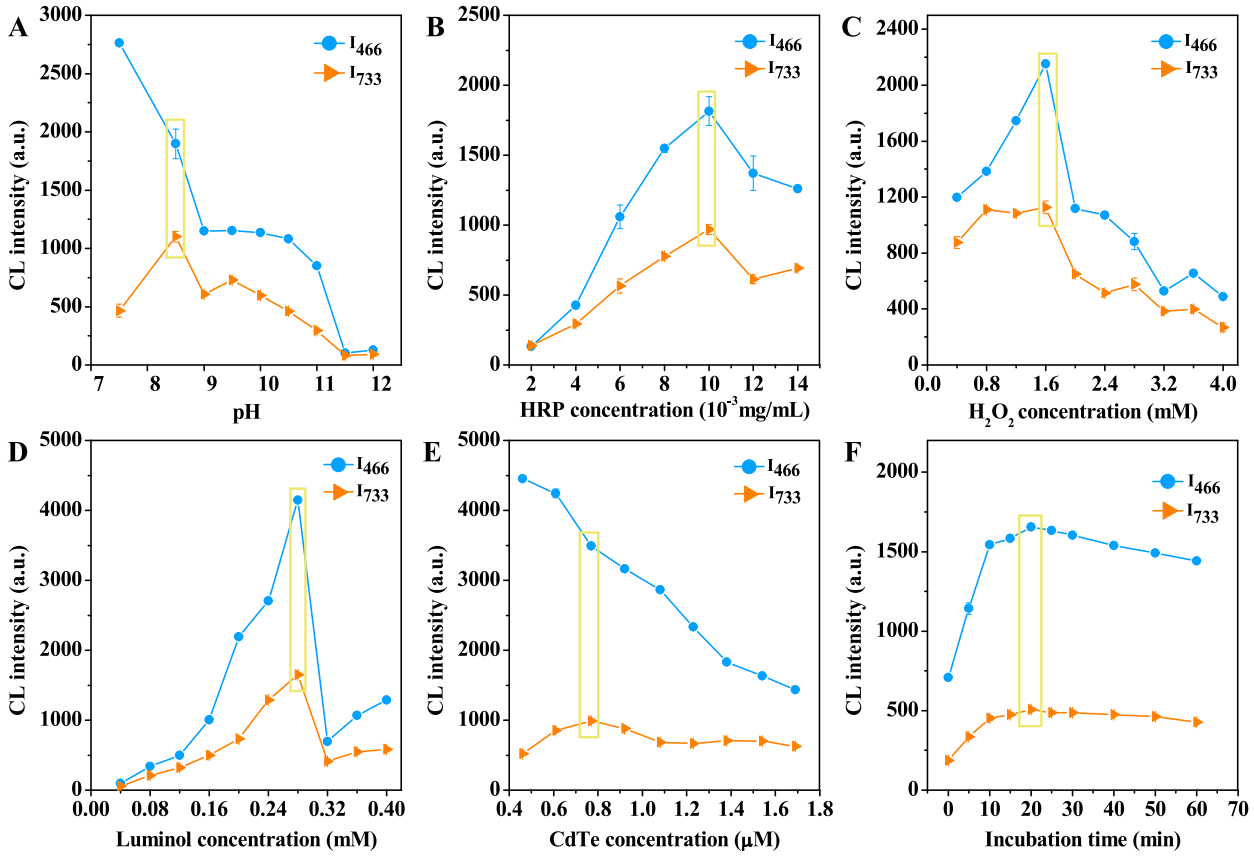

Fig. 4. Influence of pH (A), HRP concentration (B), H_2O_2 concentration (C), luminol concentration (D), CdTe QDs concentration (E) and incubation times (F).

(Shanghai, China). Standard solutions of metal ions (K^+, Li^+, Pb^{2+}, Mg^{2+}, Na^+, Hg^{2+}, Cd^{2+}, Al^{3+}, Ni^{2+}, Ca^{2+}, Zn^{2+}, Ag^+, Fe^{2+}, Ba^{2+}, Fe^{3+}, Mn^{2+}, Co^{2+}, and Cu^{2+}) were purchased from National Standard Research Center (China). Other chemicals in this work were provided by Beijing Chemical Works. 10 mM luminol stock solution was obtained by dissolving luminol solid powder with 0.1 M NaOH and stored in a dark room for a while.

2.1.2. Apparatus

The fluorescence spectra of CdTe QDs and the CL spectra of the experiment were acquired by an F-7000 fluorescence spectrophotometer (Hitachi, Japan) with the Xe lamp off. The absorption spectrum of CdTe QDs was captured by U-5100 UV/VIS spectrofluorometer (Hitachi, Japan). JEM2100F transmission electron microscopy (TEM, JEOL. Co., ltd, Japan) was used to investigate the morphology of CdTe QDs. X-ray diffraction (XRD) pattern of CdTe QDs was carried out using a 6100Lab

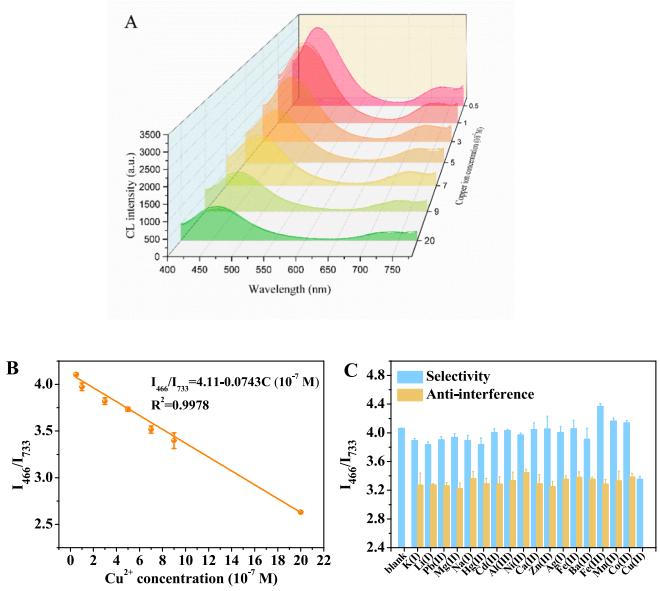

Fig. 5. (A) The curve of CL signal intensity as a function of Cu^{2+} ion concentration (0.5×10^{-7} M–20×10^{-7} M). (B) Calibration curve of ratio chemiluminescence probe for Cu^{2+} detection (0.5×10^{-7} M–20×10^{-7} M). (C) Selectivity and anti-interference assay of the ratio chemiluminescence probe (Cu^{2+}: 5×10^{-7} M, other ions: 5×10^{-6} M).

Table 1
The results of this probe to detect Cu^{2+} in tap water and lake water samples (n = 3).

Samples	Found (10^{-7} M)	Spiked (10^{-7} M)	Detected (10^{-7} M)	RSD (%)	Recovery (%)
Tap water	0	3.0	3.1	4.9	104.7
		5.0	5.2	5.4	103.2
		7.0	6.7	2.0	96.1
Lake water	0	3.0	3.0	4.5	98.7
		5.0	5.1	7.9	102.3
		7.0	7.7	6.3	109.6

diffractometer (Shimadzu). The Fourier transform infrared (FT-IR) spectrum of CdTe QDs was collected on a ThermoFisher Nicolet iS5 spectrometer.

2.2. Preparation of CdTe QDs

CdTe QDs were prepared by hydrothermal method referring to previous literature [7]. The specific steps are as follows: Firstly, to prepare NaHTe (solution A), 12.76 mg Te powder and 18.90 mg $NaBH_4$ were mixed in 1.5 mL solvent containing 0.5 mL water and 1.0 mL ethanol (V_{water}:$V_{ethanol}$: =1:2), stirred in a water bath at 60 ℃ under the protection of nitrogen. Subsequently, the black powder gradually dissolved into a brown-black solution and then the solution turned to purple, finally to a colorless solution with a few white crystals. Secondly, solution B was prepared by mixing 68.50 mg $CdCl_2$•5/2H_2O and 81.60 mg NAC in 48.5 mL deionized water (adjusted to pH = 9 with 0.2 M NaOH), and stirred vigorously in the N_2 atmosphere for 30 min. Next, the newly prepared solution A was soon injected into solution B, and the solution turned orange-red. Finally, the orange-red solution was transferred to Teflon lined stainless steel autoclave and heated at 150 ℃ for two hours to obtain the clarified CdTe QDs. The final molar ratio of Cd^{2+}/Te^{2-}/NAC was 3:1:5. Based on the previous work [23] and the first exciton absorption peak wavelength of CdTe QDs at 633 nm (Fig. 2**A**), the calculated molar extinction coefficient was 1.94×10^5 cm^{-1} M^{-1}, and the concentration of CdTe QDs prepared by us can be calculated to be 3.84×10^{-6} M.

2.3. CL measurement procedure

For the detection of Cu^{2+}, 10 μL Cu^{2+} with different concentrations was incubated with 100 μL CdTe QDs (0.77 μM) for 20 min. Then add 50 μL luminol (2.8 mM), 50 μL H_2O_2 (16 mM), 240 μL Britton–Robinson (BR) buffer solution (pH = 8.5), and 50 μL HRP (0.1 mg/mL) to the solution. Ten minutes later, the F-7000 fluorescence spectrophotometer (Hitachi, Japan) recorded the CL signal with the Xe lamp turned off.

2.4. Tap water and lake water real-samples test

The tap water and lake water were selected as practical samples to verify the practicality of the ratio detection system. Firstly, particulate matter in water samples was removed through a 0.22 μm membrane filter before use. Then incubate 10 μL tap water or lake water with 100 μL CdTe QDs (0.77 μM) for 20 min. Finally, the concentration of Cu^{2+} in actual water samples was measured as the "CL measurement procedure" described.

3. Results and discussion

3.1. Characterization of CdTe QDs

CRET efficiency can be obtained by the formula $\eta = A\ (a) / (A\ (a) + A\ (d)) \times 100$ %, where *A (a)* and *A (d)* correspond to the integral areas of receptor and donor emission respectively [7]. When 0.28 mM luminol and 0.77 μM CdTe QDs were used, the CRET efficiency was 14.59 %± 0.59 %. When the concentration of CdTe QDs was increased to 1.54 μM and 2.30 μM, the corresponding CRET efficiency is 28.48 %± 0.54 % and 40.19 %± 0.10 %, respectively. As the concentration of CdTe QDs increases, CRET efficiency tends to increase. Of course, considering the cost and effect of the experiment, the concentration of CdTe QDs should not be too high.

The TEM image of CdTe QDs is shown in Fig. 1 and the morphology of the CdTe QDs is observed. The distribution of CdTe QDS is uniform, and the average size of the obtained CdTe QDS is less than 5 nm, which is similar to the reported.

The quantum size effect of nanoparticles affects the blue shift of band absorption spectrum and fluorescence spectrum, so the absorption spectrum and fluorescence spectrum of nanoparticles have important significance for understanding the size distribution and surface structure

Table 2
Comparison with previous detection methods of Cu^{2+}.

Methods	Materials	Linear range (10^{-7} M)	LOD (nM)	Reference
Fluorescence	Graphene quantum dots (GQDs)	0–150	226	[29]
Fluorescence	CDs	0–30	35.2	[30]
Colorimetry	Carrageenan- AgNPs	25–1×10^4	1.7×10^3	[31]
Ratio fluorescence	SiNPs	0.25–200	8	[32]
Fluorescence	CdTe QDs	0.1–10	2.3	[13]
Chemiluminescence	CdTe QDs	0.7–50	40	[15]
Ratio Chemiluminescence	CdTe QDs	0.5–20	8.4	This work

of nanoparticles. Fig. 2**A and 2B** show the typical absorption and fluorescence spectra of CdTe QDs with distinct absorption and emission peaks, respectively, indicating a high monodisperse property of the CdTe QDs [24]. As shown in Fig. 2**A**, the first exciton absorption of CdTe QDs is at 1.96 eV (E (e v) $= h\,c/\lambda\,e$, $h = 6.626 \times 10^{-34}$, $c = 1 \times 10^{8}$ m/s, $e = 1.602 \times 10^{-19}$C, $\lambda = 633$ nm), which moves to a higher band than the CdTe body band gap (1.5 eV) [24], indicating that the nanoparticles have quantum size effect. Based on the wavelength of the first absorption peak, the particle size of CdTe QDs is estimated to be 4.04 nm [23], which corresponds to the size shown in the TEM image. Fig. 2**B** indicates the fluorescence spectra recorded for the synthesized CdTe QDs. It can be seen that the CdTe QDs prepared by us have a continuous and wide excitation spectrum (EM: 733 nm). Meanwhile, the fluorescence emission peak appears at 733 nm when excited in the range of 400–500 nm, that is, the fluorescence emission peak does not depend on the excitation wavelength, and 450 nm is the best excitation wavelength. At the same time, we have found that when the mixed solvent of water and ethanol is used as the reaction solvent to compare with only using water as the reaction solvent, the UV–vis absorption peak (Fig. 2**A**) and fluorescence emission peak (Fig. 2**B**) of CdTe QDs have the redshift. And the absorption peak and fluorescence emission peak of CdTe QDs shifted to long wave by 216 nm and 175 nm, respectively, implying the particle size in the mixed solvent of water and ethanol was larger. Fig. 2**C** shows the XRD pattern of CdTe QDs. The characteristic diffraction peaks appear at 25.649°, 28.428°, 31.770°, 66.267°, and 75.350°, corresponding to the crystal planes [1 1 1,2 0 0,2 1 0,4 2 0], and [5 0 0] of CdTe crystal system respectively, which comes from the card library PDF − 4 + 2009 (PDF # 01–089 − 3011), approving the synthesis of crystalline CdTe QDs. Fig. 2**D** comprises the FT-IR absorption spectrum of CdTe QDs. 3430 cm^{-1} is connected to the stretching vibration of N—H of the secondary amine of NAC, which is the characteristic frequency of amide. 2922 cm^{-1} and 1384 cm^{-1} belong to the stretching vibration and bending vibration of C—H respectively. 1632 cm^{-1} is assigned as the stretching vibration of C═O, which is the amide I band. 1543 cm^{-1} (amide II band) and 672 cm^{-1} are due to in-plane bending vibration and out-plane bending vibration of N—H, respectively. 1270 cm^{-1} is produced by stretching vibration of C—N, which is the amide III band. Also, 1047 cm^{-1} and 1086 cm^{-1} are related to C—O stretching vibrations. The spectral band of S—H appears in 2600–2500 cm^{-1}, which is sharp and easy to identify. However, the characteristic frequency of S—H is not observed in the FT-IR absorption spectra, indicating that NAC plays the stabilizing role through the interaction of S—H with Cd^{2+}.

3.2. Principle for Cu^{2+} detection

The occurrence of chemiluminescence resonance energy transfer (CRET) requires two conditions: first, the CL spectrum of the CL substrate (donor) overlaps effectively with the absorption spectrum of the acceptor; second, the spatial distance between donor and acceptor is close enough [25]. As shown in Fig. 3**A**, CL emission bands of luminol ranged from 360 to 600 nm and overlapped with the absorption bands of CdTe QDs. Meanwhile, it is known that the CRET efficiency of our system is 14.59 %, and the Forster distance of the luminol-H_2O_2-QDs CRET system is estimated to be in the range of 3–3.5 nm [6,26], so we can calculate the geometric distance between luminol and QDs to be in the range of 4.0–4.7 nm. Therefore, the system satisfies the condition of CRET, suggesting that CRET could occur between CdTe QDs and luminol.

To show that the signal at 733 nm is indeed the CdTe QDs CL peak obtained by CRET, rather than the REDOX of H_2O_2 and CdTe QDs. The luminol-H_2O_2, CdTe QDs-H_2O_2, and luminol-CdTe QDs-H_2O_2 systems were compared. And Fig. 3**B** is what we got. It can be seen that the CL signal peak of luminol appears at 425 nm for the luminol-H_2O_2 system and two CL signal peaks appear for the luminol-CdTe QDs-H_2O_2 system, but no CL signal is observed for CdTe QDs-H_2O_2 system. On the other hand, from this part of the experiment, we also found that after the addition of CdTe QDs, the peak position of luminol occurs redshift to 466 nm, and the peak intensity decreases sharply. All this is because CRET occurs between luminol and CdTe QDs, which quenches the CL signal of luminol as a donor. Finally, as shown in Fig. 3**B**, it is observed that there is no significant difference in CL intensity after adding Cu^{2+} to the luminol-H_2O_2 system, but after adding Cu^{2+} to the luminol-CdTe QDs-H_2O_2 system, CL intensity decreases greatly. This phenomenon indicates that the CL quenching is due to the interaction between Cu^{2+} and CdTe QDs. On the other hand, based on the Irving-William sequence, it was found that the paramagnetic ion Cu^{2+} generally binds more strongly than the diamagnetic ion Cd^{2+}. So, we can infer that Cu^{2+} binds to the S—H group on the surface of CdTe QDs, resulting in surface defects of CdTe QDs and CL signal quenching (Scheme 1). Meantime, the relative metal-sulfide bond strength can be measured by the respective bond energy, and the bond energy of Cu-S (274.5 ± 14.6 kJ mol^{-1}) is bigger than that of Cd-S (208.5 ± 20.9 kJ mol^{-1}) [27]. Therefore, we propose that Cu^{2+} preferentially binds to the S—H group of the stabilizer NAC on the surface of CdTe QDs and removes the S—H group from CdTe QDs, bringing about CL signal quenching.

3.3. Optimization of experimental conditions

The sensor parameters of Cu^{2+} were optimized to get better experimental results. Firstly, the pH of the system was optimized in Fig. 4**A**. It can be seen that the signal at 466 nm decreases rapidly with the increase of pH, followed by a signal plateau, and slowly decrease ensued. As the increase of pH value, the CL signal at 733 nm first increased and then basically decreased. The peak of luminol appears at 466 nm, and it is well known that alkaline conditions are favorable for luminol emission, that is, the peak at 466 nm should rise gradually with the increase of pH, while it is the opposite in this system. This phenomenon occurs because the higher the pH, the more favorable CRET occurs between luminol and CdTe QDs, and the CL intensity of the luminol as the donor decreased. Meanwhile, the CL signal peak of CdTe QDs was spotted at 733 nm, and it can be observed that the CL intensity of CdTe QDs yields the strongest emission at pH = 8.5, indicating that pH = 8.5 is the most conducive to the CL emission of CdTe QDs, so the buffer solution with pH = 8.5 was applied in subsequent experiments.

Subsequently, the effects of the concentrations of HRP, H_2O_2, luminol, and CdTe QDs were also studied. For the concentrations of HRP, the CL signals at 466 nm and 733 nm are almost synchronous (Fig. 4**B**). Initially, the CL signals gradually rise with the concentrations of HRP increasing, and the maximum CL signal occurs when the concentration of HRP is 10×10^{-3} mg/mL. After that, the intensity of CL decreases when the concentration of HRP is higher than 10×10^{-3} mg/mL. Therefore, 10×10^{-3} mg/mL HRP was used to complete the following experiments. Fig. 4**C** demonstrates the optimized data of H_2O_2 concentration. It can be seen that when the H_2O_2 concentration is 1.6 mM, the CL signals at 466 nm and 733 nm reach the maximum. In Fig. 4**D**, the trend of the signal intensity as a function of luminol concentration can be observed. The optimal concentration of luminol is 0.28 mM. The optimized data graph of CdTe QDs concentration is shown in Fig. 4**E**. As the concentration of CdTe QDs increases, CL signal intensity of luminol at 466 nm gradually decreases, which is due to the occurrence of CRET and the increase of the CdTe QDs concentration as the receptor, growing the light quenching degree of luminol as the donor. However, the CL signal of CdTe QDs at 733 nm increased at the beginning, then decreased with the increase of CdTe QDs concentration, and finally remained in a stable state. The maximum value appears when the concentration of CdTe QDs is 0.77 μM. To sum up, 10×10^{-3} mg/mL HRP, 1.6 mM H_2O_2, 0.28 mM luminol as well 0.77 μM CdTe QDs were chosen by taking the CL intensity of luminol and CdTe QDs into consideration.

Finally, the incubation duration of Cu^{2+} and CdTe QDs was studied. In Fig. 4**F**, during the first 20 min of incubation, the CL signal at 466 nm or 733 nm increased superbly with the extension of incubation time. However, after more than 20 min, the CL signal intensity at 466 nm and

733 nm CL began to decrease slowly. Therefore, an incubation time of 20 min was adopted.

3.4. Determination of Cu^{2+} using the ratio chemiluminescence probe

To evaluate the sensitivity of the ratio chemiluminescence probe toward different concentrations of Cu^{2+}, I_{466}/I_{733} signal intensity was monitored under optimal conditions, where I_{466} and I_{733} represent the CL signal intensity of this CRET system at 466 nm and 733 nm, respectively. Fig. 5**A** shows the curve of CL signal intensity as a function of Cu^{2+} ion concentration. Meanwhile, it can be observed that the Cu^{2+} concentration in the range of 0.5×10^{-7}-20×10^{-7} M has a good linear relationship with I_{466}/I_{733} (Fig. 5**B**). And the limit of detection (LOD) of Cu^{2+} was calculated (S/N = 3) to be 8.4 nM. It can be found that the chemiluminescence ratio probe has the advantages of high sensitivity, low limit of detection as well as good linear range.

3.5. Selectivity and anti-interference study of the ratio chemiluminescence probe

The response to some potential interference metal ions with concentrations of 5×10^{-6} M and 5×10^{-7} M Cu^{2+} was investigated for evaluating the specificity of this probe. As shown in the Fig. 5**C**, the CL signal intensity of Cu^{2+} is significantly lower than that of other ions, while the signal intensity of other ions is equivalent to that of the blank group, indicating that Cu^{2+} has an obvious quenching effect on the system and the system has a good selectivity to Cu^{2+}. Some potential interference ions with concentrations of 5×10^{-6} M and 5×10^{-7} M Cu^{2+} were added to the system at the same time for estimating the anti-interference of this sensor, and the CL signal was obtained in Fig. 5**C**. It has no significant difference in signal intensity between the group with other ions and Cu^{2+} and the group with only Cu^{2+}. This part of the experiment shows that the ratio detection system of Cu^{2+} established by us has a good anti-interference ability. Many previous reports have shown that Pb^{2+}, Hg^{2+}, and Ag^{+} also have a quenching effect on the fluorescence of CdTe QDs [13–15], but in this work, there is no interference. Based on the mechanism of Cu^{2+} binding to S—H to explain this phenomenon, some studies have shown that Pb^{2+} does not bind to S—H obviously, and pH has a great influence on the binding of metal cations to S—H [28]. Cu^{2+} is easier to bind to S—H than Hg^{2+} under alkaline conditions [28]. In addition, most of the studies on the interaction of Ag^{+} with CdTe QDs are under acidic and neutral conditions [9,12–14], and we speculate that Ag^{+} interacts with CdTe QDs more easily under acidic and neutral conditions, but does not bind S—H more easily than Cu^{2+} under alkaline conditions. We also find that the bond energies of Hg-S (217.3 ± 22.2 kJ mol^{-1}) and Ag-S (216.7 ± 14.6 kJ mol^{-1}) are smaller than those of Cu-S (274.5 ± 14.6 kJ mol^{-1}) [27]. Meanwhile, some studies have shown that the large size of CdTe QDs has a good selectivity for Cu^{2+} [22], and the size of CdTe QDs synthesized by us is large (4.04 nm), which is also an important factor for the good selectivity of this system.

3.6. Analysis of Cu^{2+} in tap water and lake water samples

The application value of this probe in the complex environment was explored by using tap water and lake water as the measured object, and the spiked recovery experiment was performed. The tap water and lake water samples were filtered by a 0.22 μm membrane before detection. Meanwhile, 3×10^{-7} M, 5×10^{-7} M, and 7×10^{-7} M Cu^{2+} standard solutions were added to tap water and lake water samples to conduct the spiked recovery research. All data shown in Table 1 were based on triplicate measurements. The recoveries of Cu^{2+} were 96.1 %-104.7 % in tap water and 98.7 %-109.6 % in lake water. Furthermore, the results of the comparison of the sensor's Cu^{2+} detection performance with previous analytical methods are summarized in Table 2. It was found that the detection limit of this ratio probe was lower by comparison with fluorescence and colorimetric methods. Although ratio fluorescence and fluorescence using CdTe QDs have a lower detection limit, it is inevitably affected by the scattering of background light, which reduces the experimental accuracy. However, ratio chemiluminescence can completely avoid this shortcoming.

4. Conclusion

In general, we synthesized water-soluble CdTe QDs with longer emission wavelengths and established a Cu^{2+} ratio detection system based on CRET. Herein, Cu^{2+} could combine with the S—H in the surface stabilizer of CdTe QDs, leading to surface defects of CdTe QDs and CL quenching. Meantime, based on the higher thermodynamic affinity and faster chelation process between the S—H on the surface of CdTe QDs and Cu^{2+}, the detection of the Cu^{2+} system established by us has higher selectivity and anti-interference. In addition, the ratio detection of the Cu^{2+} system we proposed has good linearity in the range of 0.5×10^{-7} M−20×10^{-7} M, and the limit of detection can be as low as 8.4 nM. The application of the ratio probe in the detection of Cu^{2+} in tap water and lake water is not only efficient, and simple, but also highly specific and is expected to detect Cu^{2+} in other practice environments.

CRediT authorship contribution statement

Xiaomin Liu: Conceptualization, Formal analysis, Investigation, Methodology, Writing - original draft. **Xinghua Wang:** Visualization, Writing - review & editing. **Ming Li:** Visualization, Writing - review & editing. **Pinyi Ma:** Visualization, Writing - review & editing. **Daqian Song:** Visualization, Writing - review & editing. **Qiang Fei:** Conceptualization, Resources, Supervision, Writing - review & editing.

Declaration of Competing Interest

The authors declare that they have no known competing financial interests or personal relationships that could have appeared to influence the work reported in this paper.

Data availability

Data will be made available on request.

Acknowledgements

The research is financially supported by the Natural Science Foundation of Jilin Province, China (No. 20210101118JC).

References

[1] R. Wang, N. Yue, A. Fan, Nanomaterial-enhanced chemiluminescence reactions and their applications, Analyst 145 (2020) 7488–7510.
[2] M.X. Sun, Y.Y. Su, Y. Lv, Advances in chemiluminescence and electrogenerated chemiluminescence based on silicon nanomaterials, Luminescence 35 (2020) 978–988.
[3] M. Hosseini, M.R. Ganjali, Z. Vaezi, B. Arabsorkhi, M. Dadmehr, F. Faridbod, P. Norouzi, Selective recognition histidine and tryptophan by enhanced chemiluminescence ZnSe quantum dots, Sens. Actuators B 210 (2015) 349–354.
[4] Y.X. Lan, F. Yuan, T.H. Fereja, C. Wang, B.H. Lou, J.P. Li, G.B. Xu, Chemiluminescence of Lucigenin/Riboflavin and Its Application for Selective and Sensitive Dopamine Detection, Anal. Chem. 91 (2018) 2135–2139.
[5] X. Huang, J. Song, B.C. Yung, X. Huang, Y. Xiong, X. Chen, Ratiometric optical nanoprobes enable accurate molecular detection and imaging, Chem Soc Rev 47 (2018) 2873–2920.
[6] Y.M. Xiong, L.H. Zhou, X.X. Peng, H.L. Li, H. Wang, L.L. He, P.L. Huang, A specific short peptide-assisted enhanced chemiluminescence resonance energy transfer (CRET) for label-free and ratiometric detection of copper ions in complex samples, Sens. Actuators B 320 (2020).
[7] S.X. Xu, X.M. Li, C.B. Li, J.L. Li, X.F. Zhang, P. Wu, X.D. Hou, In Situ Generation and Consumption of H_2O_2 by Bienzyme-Quantum Dots Bioconjugates for Improved Chemiluminescence Resonance Energy Transfer, Anal Chem 88 (2016) 6418–6424.

[8] Y.Y. Su, D.Y. Deng, L.C. Zhang, H.J. Song, Y. Lv, Strategies in liquid-phase chemiluminescence and their applications in bioassay, TrAC Trends Anal. Chem. 82 (2016) 394–411.
[9] X. Wang, W.L. Chen, H.Y. Yang, X.L. Zhang, M. Deng, X.Y. Zhou, K. Huang, P. P. Chen, B.W. Ying, Multimode detection of β-glycosidase and pathogenic bacteria via cation exchange assisted signal amplification, Microchim. Acta 187 (2020) 453.
[10] X. Wang, X. Chen, R.H. Zhou, P.Y. Hu, K. Huang, P.P. Chen, Filter-Assisted Separation of Multiple Nanomaterials: Mechanism and Application in Atomic/Mass Spectrometry/Fluorescence Label-Free Multimode Bioassays, Anal. Chem. 93 (2021) 3889–3897.
[11] K. Huang, W.Q. Deng, R. Dai, X. Wang, Q. Xiong, Q.Q. Yuan, X. Jiang, X. Yuan, X. L. Xiong, Ultrasensitive speciation analysis of silver ions and silver nanoparticles with a CdSe quantum dots immobilized filter by Cation exchange reaction, Microchem. J. 135 (2017) 74–80.
[12] R. Jian, K.L. Hu, Q. Guo, L. Zhao, H.M. Yu, K. Huang, Speciation analysis of silver ions and silver nanoparticles in commercial antibacterial products by a self-constructed fluorescent spectrophotometer, Microchem. J. 175 (2022).
[13] X. Zhao, J. Du, Y.Z. Wu, H.Z. Liu, X.P. Hao, Synthesis of highly luminescent POSS-coated CdTe quantum dots and their application in trace Cu^{2+} detection, J. Mater. Chem. A 1 (2013).
[14] T.T. Gong, J.F. Liu, X.X. Liu, J. Liu, J.K. Xiang, Y.W. Wu, A sensitive and selective sensing platform based on CdTe QDs in the presence of l-cysteine for detection of silver, mercury and copper ions in water and various drinks, Food Chem 213 (2016) 306–312.
[15] Z. Sheng, H. Han, J. Liang, The behaviors of metal ions in the CdTe quantum dots-H2O2 chemiluminescence reaction and its sensing application, Luminescence 24 (2009) 271–275.
[16] L. Liu, Q. Ma, Y. Li, Z. Liu, X. Su, Detection of biothiols in human serum by QDs based flow injection "turn off-on" chemiluminescence analysis system, Talanta 114 (2013) 243–247.
[17] Y.R. Ma, H.Y. Niu, X.L. Zhang, Y.Q. Cai, Colorimetric detection of copper ions in tap water during the synthesis of silver/dopamine nanoparticles, Chem. Commun 47 (2011) 12643–12645.
[18] K. Rurack, Flipping the light switch 'ON' — the design of sensor molecules that show cation-induced fluorescence enhancement with heavy and transition metal ions, Spectrochim. Acta A 57 (2001) 2161–2195.
[19] Z.X. Wang, Q.L. Li, F.Y. Kong, W. Wang, S.N. Ding, Picomolar Level Detection of Copper(II) and Mercury(II) Ions Using Dual-Stabilizer-Capped CdTe Quantum Dots, Journal of Analysis and Testing 2 (2017) 90–97.
[20] H. Irving, R.J.P. Williams, The stability of transition-metal complexes, J. Chem. Soc. 3192–3210 (1953).
[21] J.F. Callan, R.C. Mulrooney, Luminescent detection of Cu(II) ions in aqueous solution using CdSe and CdSe-ZnS quantum dots functionalised with mercaptosuccinic acid, physica status solidi c 6 (2009) 920–923.
[22] Y.S. Xia, C. Cao, C.Q. Zhu, Selective Detection of Mercury(II) and Copper(II) Based on the Opposite Size-dependent Fluorescence Quenching of CdTe Quantum Dots, Chin. J. Chem . 25 (2007) 1836–1841.
[23] W.W. Yu, L.H. Qu, W.Z. Guo, X.G. Peng, Experimental Determination of the Extinction Coefficient of CdTe, CdSe, and CdS Nanocrystals, Chem. Mater. 15 (2003) 2854–2860.
[24] L.H. Zhang, L. Shang, S.J. Dong, Sensitive and selective determination of Cu^{2+} by electrochemiluminescence of CdTe quantum dots, Electrochem. Commun. 10 (2008) 1452–1454.
[25] X.M. Liu, Q. Fan, X.X. Zhang, M. Li, Y.H. Huan, P.Y. Ma, D.Q. Song, Q. Fei, A FeS_2NPs-Luminol-MnO_2NSs system based on chemiluminescence resonance energy transfer platform for sensing glutathione, Talanta 240 (2022), 123171.
[26] R. Freeman, X.Q. Liu, I. Willner, Chemiluminescent and chemiluminescence resonance energy transfer (CRET) detection of DNA, metal ions, and aptamer-substrate complexes using hemin/G-quadruplexes and CdSe/ZnS quantum dots, J Am Chem Soc 133 (2011) 11597–11604.
[27] Y.R. Luo, J.A. Kerr, Bond dissociation energies, CRC handbook of chemistry and physics 89 (2012) 89.
[28] L.F. Wang, H.J. Liu, Aisanjiang·Abibu, Preliminary Study on Reactions of Sulfhydryl Group with Cu^{2+}, Hg^{2+}, Pb^{2+} and Arsenides, Endemic Diseases Bullet In 14 (1999).
[29] F.X. Wang, Z.Y. Gu, W. Lei, W.J. Wang, X.F. Xia, Q.L. Hao, Graphene quantum dots as a fluorescent sensing platform for highly efficient detection of copper(II) ions, Sens. Actuators B 190 (2014) 516–522.
[30] X.J. Liu, N. Zhang, T. Bing, D.H. Shangguan, Carbon dots based dual-emission silica nanoparticles as a ratiometric nanosensor for Cu(2+), Anal Chem 86 (2014) 2289–2296.
[31] Y.H. Wang, X.Y. Dong, L. Zhao, Y. Xue, X.H. Zhao, Q. Li, Y.Z. Xia, Facile and Green Fabrication of Carrageenan-Silver Nanoparticles for Colorimetric Determination of Cu(2+) and S(2), Nanomaterials (Basel) 10 (2020).
[32] Y.X. Yang, L. Li, L.Y. Lin, X.F. Wang, J.W. Li, H. Liu, X.F. Liu, D.Q. Huo, C.J. Hou, A dual-signal sensing strategy based on ratiometric fluorescence and colorimetry for determination of Cu(2+) and glyphosate, Anal Bioanal Chem 414 (2022) 2619–2628.